[17]C. N. Yang, Rev. Mod. Phys. 34, 694 (1962).
[18]M. E. Rensink, Ann. Phys. (N. Y.) 44, 105 (1966).
[19]T. M. Rice, Phys. Rev. 140, 1889 (1965).
[20]P. C. Hohenberg, Phys. Rev. 158, 383 (1967).
[21]Yu. A. Firsov, Proceedings of the VIIth Winter School, A. F. Ioffe Phys. Tech. Inst., 1975, p. 286.
[22]L. D. Landau and E. M. Lifshitz, Élektrodinamika sploshnykh sred (Electrodynamics of continuous media) Gostekhizdat, 1957, p. 317 [English translation published by Pergamon, Oxford].
[23]I. G. Lang and Yu. A. Firsov, Zh. Eksp. Teor. Fiz. 43, 1843 (1962) [Sov. Phys. JETP 16, 1301 (1963)].

Translated by D. ter Haar

Energy spectrum of acceptors in germanium and its response to a magnetic field

E. M. Gershenzon, G. N. Gol'tsman, and M. L. Kagane

V. I. Lenin State Pedagogical Institute
(Submitted July 12, 1976)
Zh. Eksp. Teor. Fiz. 72, 1466–1479

We investigated the spectrum of the submillimeter photoconductivity of p-Ge at helium temperatures and the effects of a magnetic field up to 40 kOe on the spectrum. A large number of lines of transitions between the excited states of the acceptors was observed, some of the lines were identified, and the energies of a number of spectral levels B, Al, Ga, In, and Tl in Ge were identified. The results are compared with calculations and with experimental data obtained from the spectra of the photoexcitation of the ground state of the impurities. Using one transition as an example, we discuss the splitting of the excited states of acceptors in the magnetic field and under uniaxial compression.

PACS numbers: 72.40.+w, 71.70.Ej

INTRODUCTION

Besides the study of the energy spectrum of donors in semiconductors,[1] great interest attaches to an investigation of shallow acceptors. This, however, is a more difficult task both theoretically and experimentally. The calculation of the acceptor spectrum in Ge by the effective-mass method[2–5] and the study of the effect of a magnetic field and of uniaxial deformation of the sample on this spectrum within the framework of perturbation theory[6–12] is quite complicated. It has been carried out for a limited number of states and yields less reliable results than in the case of donors (e.g.,[13–15]). A group-theoretical analysis of the influence exerted on the spectrum by a magnetic field[16] and by uniaxial deformation (F)[17] yields new information and a number of exact results, but is not sufficient.

The spectrum of acceptors of group III in Ge was experimentally investigated with long-wave infrared grating spectrometers with registration of the absorption of the radiation,[12,18–22] including studies in the presence of a field H and a deformation F and photoconductivity,[23,24] and also with Fourier-transformation spectrometers with registration of the photoconductivity.[25,26] Transitions from the ground state were investigated, and some of them, to the nearest excited state, could be identified with those calculated. The resolution and sensitivity of the spectrometers used in[12,20–22] were adequate for a detailed investigation of the Zeeman and piezosplitting of only an insignificant number of the spectral lines and under sufficiently strong perturbations. At the same time, the theory is applicable most fully only in the region of small perturbations.

The purpose of the present work was to study the energy spectrum of shallow acceptors in Ge, the effect exerted on this spectrum by a magnetic field, and in a number of cases the effect of uniaxial compression, by using a sensitive high-resolution submillimeter spectrometer based on backward-wave tubes (BWT). We first investigated several series of transitions between excited states of acceptors, but unfortunately, the short-wave limit of the employed spectrometer ($\lambda \approx 250$ μm) did not make it possible to study the spectrum of the transitions from the ground state. In view of the limitations of the theory the most detailed investigations of the Zeeman effect and of the effect of uniaxial compression were restricted to line splitting under small perturbations. The measurements were performed by determining the photoconductivity due to photothermal ionization[27,28] of the excited states of the impurity.

EXPERIMENTAL CONDITIONS AND PROCEDURE

The photoconductivity spectra of the acceptors in Ge were measured mainly in the same way as those of the donors.[1] However, the more complicated character of the acceptor center, and the fact that it has been less thoroughly studied, led to a number of modifications of the measurement procedure. The following factors become significant: the determination of the spectrum of the excited states at $H=0$ and its response to uniaxial compression, the study of the Zeeman effect following compression of the sample, the determination of the relative intensities of the Zeeman and piezoelectric components when various polarizations of the radiation are used, and the measurement of the anisotropy of the Zeeman effect.

 0038-5646/77/4504-0769$02.40

TABLE I. Ge samples used in the study.

Sample No.	Principal impurity	N_a, 10^{12} cm^{-3}	$K=N_a/N_d$, %	Sample No.	Principal impurity	N_a, 10^{12} cm^{-3}	$K=N_a/N_d$, %
1	B	1,5	4,9	8	Al	250	12
2	B	2,6	30	9	Al	300	0,3
3	B	3	<10	10	Ga	180	2
4	B	6	5	11	Ga	570	6
5	B	80	25	12	In	~1	–
6	B	130	27	13	In	45	30
7	Al	3	<10	14	Tl	840	3,8

We used weakly compensated p-Ge samples (Table I), the concentration of the main impurity being $N_a \approx 10^{12} - 8.5\times10^{14}$ cm^{-3}, which exceeds substantially the concentrations of the other acceptors. The samples usually were plates (4×4×2 mm) or disks (10 mm diameter, 1.5 mm height) with ohmic contacts. For experiments with uniaxial compression we used long samples (2.5 × 2.5× 24 mm); the force was applied along the longest edge.

In the Zeeman measurements, the sample was placed in a superconducting solenoid in such a way that its surface, which coincided with the crystallographic (110) plane, was parallel to **H** and perpendicular to the propagation direction of the submillimeter radiation. It was therefore possible to carry out the measurements at two polarizations of the radiation (**E** ∥ **H** and **E** ⊥ **H**) and to choose the direction of **H** along any crystallographic axis in the (110) plane. Under the conditions of uniaxial compression, the force was parallel to the magnetic field (**F** ∥ **H**).

The orientation of the sample relative to the field **H** was monitored against the position of the peaks of the photoconductivity of the cyclotron resonance (CR) of the free electrons in the spectrum, when the free electrons were generated by interband pumping with an incandescent lamp. The degree of polarization in the sample was verified against the ratio of the intensities of the CR peaks of the light electrons at **H** ∥ [111] for two orientations of the electric-field vector, **E** ∥ **H** and **E** ⊥ **H**. These measurements have shown that the employed samples cause a partial depolarization. Thus, this CR peak should not be observed at **E** ∥ **H** in the submillimeter channel, but its intensity decreased for samples by only a factor of 3–10 in comparison with the case **E** ⊥ **H**.

In measurements of the photoconductivity spectra with H scanning, the relative line intensities are usually distorted because of the change of the sample resistance in a magnetic field, since it is usually connected in the current-generator circuit. To obtain the true intensity ratio we connected in series with the sample and with a stabilized voltage source a coil having a large inductance but a small dc resistance. This circuit ensured a constant bias voltage on the sample and prevent shunting of the alternating signal.

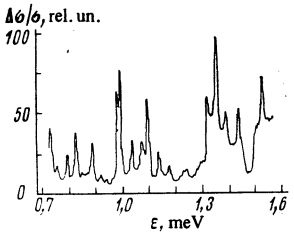

FIG. 1. Photoconductivity spectrum of Ge(B) sample No. 4 at a constant sample bias 0.5 V/cm, and $T \approx 6.5$ K. The samples are numbered here and below in accordance with Table I.

EXPERIMENTAL RESULTS

1. Figure 1 shows a typical photoconductivity spectrum of a Ge(B) sample at $H=0$, recorded at the optimal observation temperature $T \approx 6.5$ K,[1] in the emission photon energy range $\varepsilon = 0.7$–1.6 meV. Since the concentration of the acceptors is low enough, the line width is 0.006–0.014 meV, and even the closely lying lines can be easily resolved. Table II lists the entire obtained set of lines of transitions between the excited states and $H=0$ for the investigated materials at $T \approx 7$ K, with Ge(B) investigated in the greatest detail.[1)] It is seen that the energy positions of most spectral lines depend quite little on the type of impurity. The changes amount to as much as 0.2 meV for only a few lines.

In addition to the photoconductivity spectra we measured the absorption in a Ge(B) sample with $N_a \approx 10^{14}$ cm^{-3}, in the range 1.30–1.41 meV, using the procedures described in[29]. We registered one line with energy 1.365 meV.

2. Figure 2 shows typical photoconductivity spectra of Ge(B), with magnetic-field scanning, at different polarizations of the radiation. The ratio of the line intensities over a considerable number of transitions between excited states of acceptors and the resonance lines of the free holes, recorded at $\lambda = 1.17$ mm (Fig. 2a) is different for **E** ∥ **H** and **E** ⊥ **H**. The presence of a certain depolarization introduced by the sample makes it possible to reveal all the lines in one spectrum and to determine their "sensitivity" to the predominant polarization. This is illustrated, using as an example, by the Zeeman components of the intense line with energy $\varepsilon_1 = 2.435$ meV at $H=0$ (Fig. 2b), recorded at a

TABLE II. Energy (ε_T, meV) of the transitions between the excited states of impurities of group III in Ge.

Sample No.	B	Sample No.	B	Sample No.	B	Sample No.	Al	Ga	In	Tl
1	0.61	21	1.30	41	2.17	4	—	0.74	0.75	—
2	0.66	22	1.320	42	2.21	5	—	0.78	0.78	—
3	0.70	23	1.365*	43	2.35	7	0,84	0.84	0.85	—
4	0.735	24	1.390	44	2.435*	14	1,05	1.04	1.05	1.03
5	0.75	25	1.445	45	2.485	16	—	1.08	1.10	1.08
6	0.80	26	1.51	46	2.600	17	1,14	1.13	1.12	1.11
7	0.830	27	1.535*	47	2,605*	19	1,22	1.21	1.22	1.22
8	0.89	28	1.590*	48	2.865*	21	1.29	—	1.27	—
9	0.90	29	1.62	49	2,91	23	1.36*	1.29*	1.24*	1.18
10	0,92	30	1.640*	50	3,10	28	1.59*	1.60*	1.59	1.61*
11	0.94	31	1.70	51	3,260	30	1,62*	1.61*	1.62	1.63
12	0.990	32	1.730*	52	3.30	32	1.74*	1.82*	1.88*	1.93*
13	1,005*	33	1.76	53	3.370*	34	1,79	—	—	1.81
14	1,045	34	1.78	54	3,48	44	2.435*	2.43*	2.42*	2.42*
15	1.08	35	1.86	55	3,585*	45	2.485	—	2.46	—
16	1,100	36	1.90	56	3,79	47	2.63	—	2.74	—
17	1.140	37	1.935	57	3.875	48	2.86*	2.85*	2.83*	2,83*
18	1.18	38	1.995	58	3,89	51	3,25	3.25	3.25	3.24
19	1.23	39	2,035	59	3,925	52	—	—	3.28	—
20	1.25	40	2.065*	60	4.035	53	3.36*	3.36*	3.35*	3.35*
				61	4.13	55	3.58*	—	3.56*	—

*Spectral lines that are intense in comparison with the adjacent lines. For Al, Ga, In, and Tl, the spectral lines not listed in the table have energies that differ from the corresponding lines for B and Be by not more than 0.01 meV.

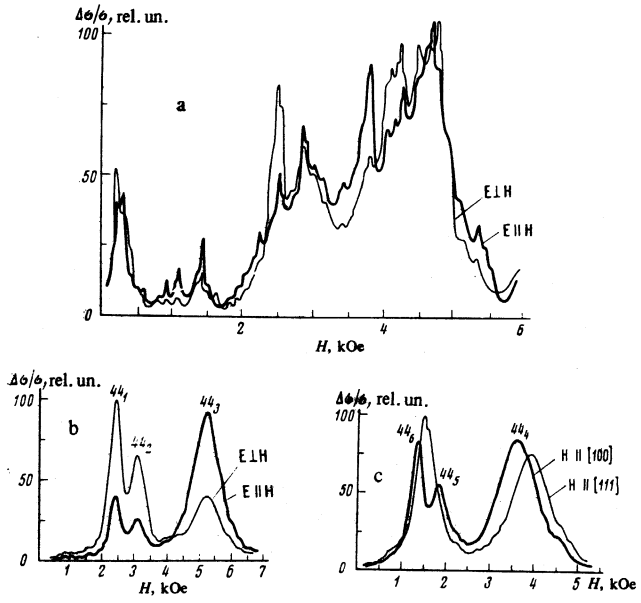

FIG. 2. Photoconductivity spectra of Ge(B) sample No. 3; $T \approx 6.5$ K, bias 0.5 V/cm. a) $\mathbf{H} \parallel [100]$, $\varepsilon = 1.065$ meV; b) $\mathbf{H} \parallel [100]$, $\varepsilon = 2.395$ meV; c) $\varepsilon = 2.465$ meV, unpolarized radiation. Here and below the lines are numbered as in Table II, while the subscript numbers the Zeeman component.

sufficiently high radiation frequency $\lambda = 0.518$ mm), at which the section of the spectrum is simpler. The use of unpolarized radiation, for which all the transitions are on a par, may in turn be useful, for example, in the measurement of the anisotropy of the Zeeman effect. Thus, one can see distinctly all three components on the curves of Fig. 2c, which were plotted for the same line ($\varepsilon_l = 2.435$) at $\lambda = 0.503$ mm, for two values of the angle α between the magnetic field and the [100] axis at $\mathbf{H} \parallel (110)$.

Figures 3 and 4 show the results of measurements of the Zeeman effect of an appreciable number of transitions at $\mathbf{H} \parallel [100]$. The figures show all the observable

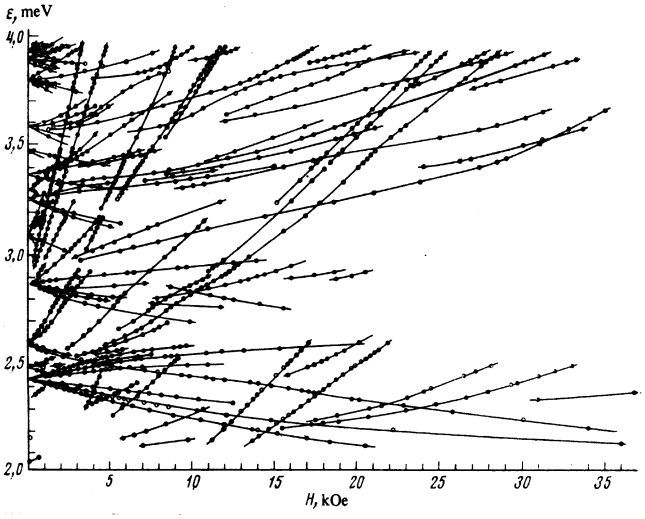

FIG. 3. Plots of $\varepsilon(H)$ for Ge(B) in the range $\varepsilon = 2.0$—4.0 meV; $\mathbf{H} \parallel [100]$, unpolarized radiation.

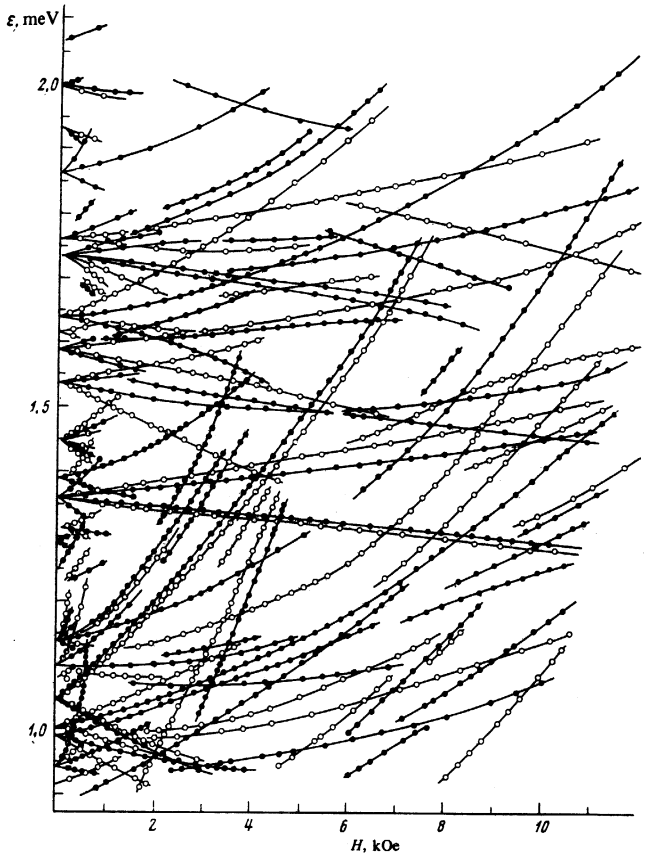

FIG. 4. Plots of $\varepsilon(H)$ for Ge(B) in the range $\varepsilon = 0.9$—2.1 meV: ● – $\mathbf{E} \perp \mathbf{H}$, ○ – $\mathbf{E} \parallel \mathbf{H}$; $\mathbf{H} \parallel [100]$.

lines that are due only to the Zeeman components, but not to quantum resonances of the free holes. The large number of lines, even larger than in the case of donors,[1] causes the weakest transitions between the excited states to be resolved only in individual sections of the spectrum.

3. Figures 5 and 6 show the results of measurements of the anisotropy of the linear Zeeman effect. The high resolution of the employed spectrometer has made it possible to observe a number of lines with 0.2–0.4 kOe in the region of their linear splitting.

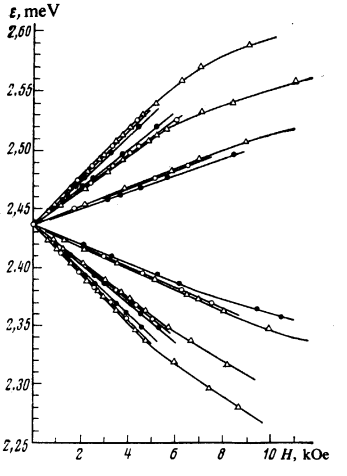

FIG. 5. Zeeman components of lines with $\varepsilon = 2.435$ meV in Ge(B) in the region of weak magnetic fields for three principal orientations: Δ – $\mathbf{H} \parallel [100]$, ● – $\mathbf{H} \parallel [111]$, ○ – $\mathbf{H} \parallel [100]$.

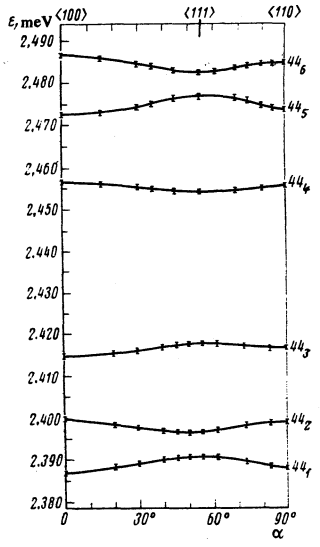

FIG. 6. Plots of $\varepsilon(\alpha)$ for the Zeeman components of the 2.435-meV line at $H = 2.42$ kOe.

Figure 5 shows the splitting of the components of the 2.435-meV transition in weak fields up to 5 kOe for the three principal orientations of the sample in the magnetic field (α is the angle between **H** and the [100] axis), **H** ∥ (110), when the Zeeman effect is still practically linear. Starting with $H = 5-7$ kOe, a positive nonlinear shift of the lower components, and a negative shift of the upper components is observed. The results, which are summaries of several runs of measurements of the anisotropy of the linear effect of all the components of this transition, are shown in Fig. 6.

For the 1.045-meV transition, the $\varepsilon(\alpha)$ dependence can be obtained from Fig. 7, which shows, in contrast to Fig. 6, the plot of $H(\alpha)$ without conversion of the data into $\varepsilon(\alpha)$ and with allowance for the linearity of the splitting. This figure shows only two components, the behavior of the others being the same.

The anisotropy of the Zeeman components of the 1.365-meV transition was investigated qualitatively and has revealed an increase of the splitting of four internal intense components with increasing α, when the sample was rotated from the position **H** ∥ [100] to **H** ∥ [111].

4. A number of transitions were investigated under uniaxial deformation of the sample. Figure 8 shows the transformation of the line $\varepsilon_1 = 2.435$ meV following application of a force along the [100] axis of the crystal, namely, two piezocomponents with different in-

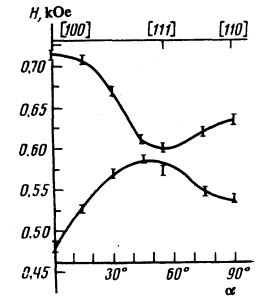

FIG. 7. Plot of $H(\alpha)$ for the components of the 1.045-meV line at $\varepsilon = 1.080$ meV.

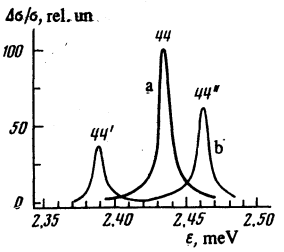

FIG. 8. Section of the photoconductivity spectrum of Ge(B) sample No. 2 at $T = 7$ K and $E = 0.5$ V/cm: a) in the absence of compression, b) at a pressure 65 kg/cm^2, **F** ∥ [100]. The prime and double prime marking the line number represents the number of the piezocomponent.

tensities are observed, and with a center of gravity that shifts towards lower energies even under a weak pressure. Figure 9 illustrates schematically the correspondence between the Zeeman and the piezocomponents. This correspondence was established by measurements of this line without pressure (a), under uniaxial compression in the absence of a magnetic field (b), under simultaneous action of pressure and a magnetic field (**F** ∥ **H**) (c), and in the absence of pressure but in the presence of H (d). The measurements have shown that transitions with energies 2.865 and 3.37 meV split at **F** ∥ [100] into four piezocomponents each.

DISCUSSION OF RESULTS

1. The fact that the calculations of the acceptor spectrum are incomplete raises considerable difficulties in the identification of the observed transitions between the excited states. A number of transitions can nevertheless be determined. Figure 10 shows by way of example the identified series of transitions following photoexcitation of different states of boron in Ge, which have been separated from a large number of observed lines (Table II). Similar series can be obtained also for other impurities. A summary of the energy levels of the shallow acceptors in Ge according to our results and the results obtained by others,[19,23,25,26] who measured transitions from the ground states, is given in Table III. The states are marked by the same symbols as in[19,25,26], for transitions from the ground state to the same excited states, but marked by an asterisk (*).

The spectrum can be analyzed because of the information obtained on the energy and intensity of the lines, their splitting in the magnetic field and under compression, from polarization-measurement data, from the anisotropy of the Zeeman effect, and from the chemical shifts of the lines. We illustrate the identification process using as an example the lines belonging to the

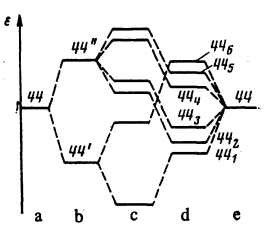

FIG. 9. Splitting of the 2.435-meV line at: a) $F = 0$, $H = 0$; b) **F** ∥ [100], $H = 0$; c) **F** ∥ **H** ∥ [100]; d) $F = 0$, **H** ∥ [100].

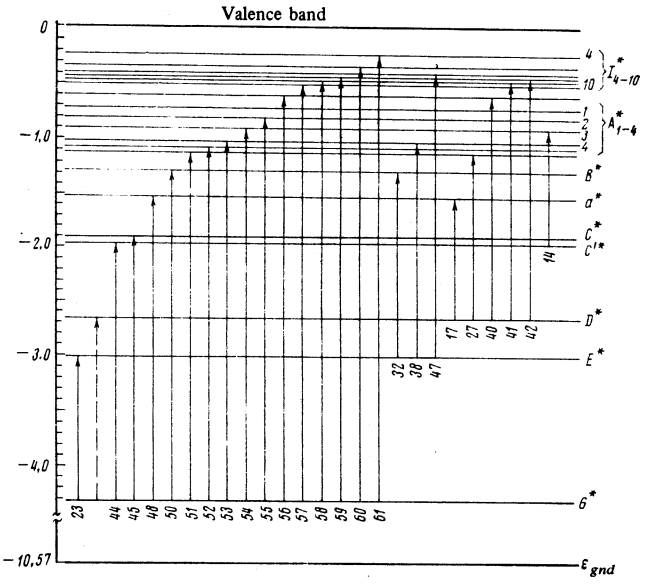

FIG. 10. Energy spectrum (the energies are in meV) of boron in Ge; the arrows mark the identified transitions, whose numbers correspond to those of Table II.

series of transitions from the first excited state G^* in Ge(B). We can ascribe to this series, first of all, the lines with energy $\gtrsim 3$ meV—the ionization energy of the second excited state E^*. A comparison of this group of lines (Fig. 10) with the published data (Table III) shows that the best agreement between the level energies is obtained when the energy of the G^* level is 4.365 meV.

A more difficult task is the determination of those transitions of this series which have energies lower than 3 meV. Thus, candidates for the $G^* \to E^*$ transitions may be the spectral lines with energies 1.32, 1.365, and 1.39 meV, which are close to the corresponding level energy difference in Table III. The $G^* \to E^*$ transition is a transition between states of different parity,[3,19] and can therefore be intense enough both in absorption spectra and in photoconductivity spectra. Experiment shows that from among the transitions listed above this condition is satisfied by the 1.365-meV transition. The corresponding transitions in Ge with other impurities (Table II) differ noticeably in energy, a fact that agrees with the chemical shift characteristic of the E^* level (Table III) and confirms the identification.

The transition $G^* \to D^*$, whose energy should be ~1.72 meV according to the published data (Table III), can correspond to the line with energy 1.73 meV. This, however, is not the case. It was established that this line is subject to a chemical shift to $\varepsilon = 1.88$ meV in Ge(In), which is close in magnitude to the shift of the $G^* \to E^*$ transition, but is of opposite sign. The line in question pertains therefore to a series of transitions from the state E^* and corresponds to the transition $E^* \to B^*$. The sought $G^* \to D^*$ transition has apparently a low intensity and is not observed in the photoconductivity spectrum (it is shown dashed in the diagram of Fig. 10). The sum of the energies of the two successive transitions $G^* \to E^*$ and $E^* \to B^*$ is 3.10 meV. The presence in the spectrum of a weak line with this energy is an additional confirmation of the identification given in Fig. 10.

We now dwell on the $G^* \to C^*$ transition, which can have an energy close to 2.47 meV (see Table III). From among the lines of the transitions between the excited states in Ge(B), two suitable lines were registered: an intense 2.435-meV line and a weak 2.485-meV line. It turns out that they correspond to transitions from the G^* state to two close levels, C^* and C'^*. Indeed, experiments in a magnetic field (Fig. 5) and under uniaxial compression of the sample (Fig. 8) reveal the interaction of the sublevels of these lines. It manifests itself in the fact that the Zeeman components of the 2.435 and 2.485 meV lines reveal, as noted earlier, a strong deviation from a linear $\varepsilon(H)$ dependence, and a substantial energy change in a field $H \geq 5$–7 kOe, while the center of gravity of the piezocomponents of the 2.435-meV line shifts towards lower energies. The interaction of the sublevels indicates that the transitions in question have one common state. When account is taken of the transition energies, this can be one of the rather deep levels: G^*, E^*, D^*, which serves as the starting state. Each of these levels has fourfold degeneracy.[3,19] The intense 2.435-meV line has at $\mathbf{H} \parallel [100]$ six Zeeman components and two piezocomponents at $\mathbf{F} \parallel [100]$ and for unpolarized radiation (Fig. 9), thus indicating, in accordance with the selection rules,[9,16,12,17] that the final state is doubly degenerate.

For a subsequent analysis it is necessary to invoke the results of the study of the transitions from the ground state[12,20,21,30] and the calculation data.[3,5] In the absorption spectrum of singly ionized zinc (Zn^-) in Ge,[30] which is analogous to the impurities of group

TABLE III. Energies (meV) of the levels of shallow acceptors in Ge, obtained from the published data (I) and from the results of the present paper (II).

State	B		Al		Ga		In		Tl	
	I	II	I	II	I	II	I	II	I	II
I_1^*	0.036	–	0.036	–	0.052	–	–	–	–	–
I_2^*	–	–	0.143	–	0.112	–	–	–	–	–
I_4^*	–	0.235	0.231	–	–	–	–	–	–	–
I_5^*	–	0.330	0.305	0.33	–	–	–	–	–	–
I_6^*	0.372	0.39	0.367	0.375	0.396	–	0.36 [23]	0.38	–	–
I_7^*	0.431	0.435	0.426	0.43	0.445	0.43	–	0.43	–	–
I_8^*	–	0.475	0.442 [26]	0.47	–	0.47	–	0.47	–	–
I_9^*	0.522	0.49	0.518	0.49	0.534	–	–	0.49	–	–
I_{10}^*	0.581	0.575	0.580	0.57	–	0.57	–	0.57	–	0.57
A_1^*	0.707	–	0.702	–	0.710	–	0.707	–	–	–
A_2^*	0.785	0.780	0.770	0.78	0.783	–	0.785	0.79	0.77 [19]	–
A_3^*	0.915	0.885	0.905	0.89	0.918	–	0.912	0.89	0.94 [19]	0.89
A_4^*	1.002	1.000	0.973	1.00	0.979	1.00	0.994	1.01	–	1.01
–	–	1.065	–	–	–	–	–	1.07	–	–
–	–	1.10	–	1.10	–	1.10	–	1.10	–	1.11
B^*	1.250	1.265	1.246	1.26	1.256	1.25	1.234	1.24	1.28 [19]	1.25
a^*	1.51 [19]	1.500	–	1.50	–	1.51	1.54 [19]	1.525	1.55 [19]	1.53
C^*	1.884	1.880	1.875	1.875	1.885	–	1.876	1.89	1.88 [19]	–
C'^*	–	1.930	–	1.925	–	1.93	–	1.93	–	1.93
D^*	2.634	2.635	2.628	2.64	2.633	2.64	2.627	2.64	2.63 [19]	2.64
E^*	3.00 [19]	3.000	–	3.00	3.05 [19]	3.07	3.32 [19]	3.12	3.37 [19]	3.18
G^*	4.355	4.365	4.335	4.36	4.35	4.36	4.35 [19]	4.355	4.33 [19]	4.355
ε_i	10.57		10.90		11.07		11.74		13.20	

Note: The differences between the ionization energies (ε_i) from[25] and the energies of the transitions from the ground and the corresponding excited states,[19,23,25,26] ε_i for Ge(Tl) was obtained in the same manner as in[25], by increasing the value of ε_i from[19] by 0.1 meV. Unless otherwise indicated, the published data are taken from[25].

TABLE IV. Linear g factors of the states (8–01) and (7–0) in Ge(B) for three directions of the magnetic field relative to the crystal axes.

States in $H=0$ (from[3])	$g_{\pm\mu}$	Orientation H∥[100]	H∥[111]	H∥[110]
(7–0)	$g_{\pm 1/2}$	+4.10	+4.10	+4.10
(8–01)	$g_{\pm 1/2}$	+3.04	+2.48	+2.86
	$g_{\pm 3/2}$	−0.37	−0.54	−0.43

III, there were observed two close transitions with final states C'^* and C^*. Although no C' line was observed in Ge with impurities of group III,[19,22,25,26] a study of the splitting of the piezocomponents of the C line has enabled the authors of[12,20,21] to observe, under conditions of uniaxial compression, the components of two states which they identified with the twofold degenerate and fourfold degenerate states calculated in[3]. According to the data of[12,21], the components of these two states interact. It was assumed in[30] that the lines C and C' in Ge with Zn^- impurity correspond to the C line in Ge with impurities of elements of group III, since these lines exhibited similar splitting under compression. Starting from the energy difference between the lines C and C' in Ge with Zn^-, an estimate was made in[30] of the possible energy difference of these lines in Ge with impurities of group III, and a value ~0.04 meV was obtained.

The lines under discussion in our spectra (44 and 45 in Table II) have thus an energy difference that is close to that predicted in[30]; the intense line 44, which has been investigated in greatest detail, has fourfold degeneracy of the starting state and twofold degeneracy of the final state. Finally, judging from the character of the interaction of these lines and from the energy values, they can be identified, taking the foregoing into account, as the transitions $G^* \rightarrow C'^*$ and $G^* \rightarrow C'$, respectively. We note that the intensity ratio of these transitions is the inverse of that of lines C' and C in[30], apparently as a result of the different parities of the starting states in these cases.

We proceed now to identification of the remaining transition $G^* \rightarrow a^*$ of the investigated series. Since these states seem to be of different parity,[12] it follows that among the lines of appropriate energy (Table III) one should consider the rather intense lines (Table II). There is only one such line, with energy 2.865 meV. Its identification as the $G^* \rightarrow a^*$ transition is additionally confirmed by the following considerations. The a^* state, just as the ground state and the E^* state of the impurity, is of the s-type.[3,12] These states are the most sensitive to the chemical nature of the impurity, and their energy increases with increasing atomic number of the impurity. The chemical shift should be larger for the higher excited states. Indeed, the final state of the considered transition in materials with different impurities undergoes the expected small chemical shift (see Table III). In addition, the splitting of this transition under uniaxial compression of the sample ($\mathbf{F} \parallel [100]$) into four piezocomponents agrees with the required fourfold degeneracy of the state a^*.

In concluding the analysis of the series of transitions from the G^* state, it should be noted that besides the transitions between states of different parities, transitions having a noticeable intensity in the photoconductivity spectra are those between states of like parity. No final states with energies 2.485, 3.26, and 3.30 meV have previously been observed for the identified transitions.

2. Having obtained definite information on the energy spectrum of the acceptors from the experimental data, let us attempt to extract information on the excited state themselves. In principle, a study of the influence of a magnetic field and of uniaxial compression makes it possible to determine the structure of the states (their g factors, the degree of degeneracy, etc.), but unfortunately the presently existing theory of acceptors limits greatly the possibility of the analysis. For example, even for weak fields, the obtained values of the g factors[6–11] are quite approximate,[22] and the absorption coefficients calculated in[9] for transitions between the Zeeman sublevels are given only for transitions from the ground state and cannot be used in the present work.

We confine ourselves here only to a preliminary discussion of the information provided the Zeeman and piezospectra, which can be obtained by using group theory.[16,17] Let us dwell on the example provided by the already discussed $G^* \rightarrow C'^*$ transition (No. 44 in Table II) in sufficiently weak fields H and at small F, when the splitting is linear and the difference between the sublevel populations is not yet significant.

As already noted, the starting state of the $G^* \rightarrow C'^*$ transition is fourfold degenerate, while the final state is twofold degenerate. Accordingly, using the terminology of[3], the transition in question is the (8–01) → (7–0) transition pertaining to the $\Gamma_8 \rightarrow \Gamma_7$ type.

Let us determine the values of the splitting and the sequence of the sublevels for (8–01) and (7–0) in a magnetic field and under pressure, i.e., respectively the

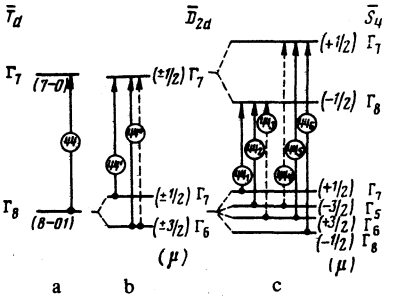

FIG. 11. Splittings of the states (8–01) and (7–1) in accordance with the notation of[3], and the observed transitions between them at: a) $F=0$, $H=0$; b) $\mathbf{F} \parallel [100]$, $H=0$; c) $\mathbf{H} \parallel [100]$, $F=0$. Solid arrows—transitions realized at $\mathbf{E} \perp \mathbf{H}, \mathbf{F}$, dashed—at $\mathbf{E} \parallel \mathbf{H}, \mathbf{F}$.

g factors and the deformation-potential constants. The results of the analysis of the experimental data are given in Table IV, which lists the g factors of the states in the three principal orientations, and in Fig. 11, which shows the splitting of the state and the transitions observed by us at $\mathbf{H} \parallel [100]$ $(44_1 - 44_6)$ in accordance with the data of Figs. 2b and 2c, and at $\mathbf{F} \parallel [100]$ $(44', 44'')$ in accordance with Fig. 8. To obtain these data we use mainly the intensity ratio and the sensitivity to the polarization of the components of the considered transition. Thus, in accordance with the theory,[16] the intensity ratio for the Zeeman components of a transition of the type $\Gamma_8 \to \Gamma_7$ at $\mathbf{H} \parallel [100]$ should be

$$(\pm 1/2 \to \mp 1/2)_\perp : (\pm 3/2 \to \pm 1/2)_\perp : (\pm 3/2 \to \mp 1/2)_\parallel = 3_\perp : 1_\perp : 4_\parallel,$$

where the symbols $\perp$ and $\parallel$ indicate the polarization of the radiation relative to the field $\mathbf{H}$ ($\mathbf{E} \perp \mathbf{H}$ and $\mathbf{E} \parallel \mathbf{H}$), which is needed for the realization of the transition. The experimentally obtained ratio is $3_\perp : 1.5_\perp : 3.5_\perp$ for the lower $(44_1, 44_2, 44_3)$ or upper $(44_6, 44_5, 44_4)$ components (see Fig. 2c), which correlates well with theory when account is taken of some overlap of the lines.

Under uniaxial compression ($\mathbf{F} \parallel [100]$), the two piezocomponents $44'$ and $44''$ (see Fig. 8) have an intensity ratio 3:5. As established by an experimental with simultaneous uniaxial compression and a magnetic field ($\mathbf{F} \parallel \mathbf{H} [100]$), the $44''$ component is actually a superposition of two transitions (see Fig. 9). The theory of[7] gives the following ratio for the intensities of the three piezocomponents in a transition of the $\Gamma_8 \to \Gamma_7$ type at $\mathbf{F} \parallel [100]$:

$$(\pm 1/2 \to \pm 1/2)_\perp : (\pm 3/2 \to \pm 1/2)_\perp : (\pm 3/2 \to \pm 1/2)_\parallel = 3_\perp : 1_\perp : 4_\parallel.$$

Since the last two transitions take place between identical sublevels, only two components with an intensity ratio 3:5 should be observed when unpolarized radiation is used, a fact that agrees well with the experimental data. This identification clarifies immediately the sequence of the sublevels of the state (8–01) (see Fig. 1b), and the deformation-potential constant of this state at $\mathbf{F} \parallel [100]$, calculated in accordance with[17], turns out to equal $b = +0.45 \pm 0.05$ eV; the values of the elastic constants were taken from[31].

To establish the sequence of the Zeeman sublevels and to obtain the g-factors of the states (7–0) and (8–01) it is necessary to resort to a number of supplementary data. For the doubly degenerate states, particularly (7–0), the Zeeman energy of a hole at a sublevel with $\mu = 1/2$ should be positive,[9] and this determines the sequence of the (7–0) sublevels. Furthermore, information for the identification of the transitions follows from the measurements of the anisotropy of the linear Zeeman effect. Indeed, if, following,[10,16] we assume that the state (7–0) makes no contribution to the anisotropy of the components of the line in question, then the anisotropic part of the Zeeman splitting of the transitions that go from two symmetrical sublevels of (8–01) into one final state, should differ only in the sign. Taking into account the selection rules, this makes it possible to separate the pair of transitions $(44_2, 44_3)$ (see Fig. 6), the starting sublevels of which we have $\mu = -3/2$ and $+3/2$, and the common final level of which has $\mu = -1/2$, as well as an analogous pair $(44_4, 44_5)$ with final $\mu = +1/2$, thereby uniquely identifying the sublevels with $\mu = +3/2$ and $\mu = -3/2$ of the state (8–01). The fact that all three upper components $(44_4, 44_5, 44_6)$ undergo a negative nonlinear shift (see Fig. 5) starting with fields ~5 kOe determines the positions and the order of the remaining sublevels of this state with $\mu = +1/2$ and $\mu = -1/2$. This means that all have a single final sublevel ($\mu = +1/2$) of the state (7–0), which is apparently the one that interacts with the higher state.

Concluding thus the brief discussion of the presented experimental data, we hope that the data on the energy spectrum of the acceptors and on the effect exerted on it by the magnetic field will stimulate a development of a theory of this question.

[1)] In measurements in which the frequency was varied (as against H scanning), allowance for the possible interference phenomena in the channel makes the fourth significant figure in the value of the transition energies uncertain.

[1] E. M. Gershenzon, G. N. Gol'tsman, and A. I. Elant'ev, Zh. Eksp. Teor. Fiz. **72**, 1062 (1977) [Sov. Phys. JETP **45**, 555 (1977)].
[2] D. Schechter, J. Phys. Chem. Solids **23**, 237 (1962).
[3] K. S. Mendelson and H. M. James, J. Phys. Chem. Solids **25**, 729 (1964).
[4] N. O. Lipari and A. Baderesehi, Phys. Rev. Lett. **25**, 1660 (1970).
[5] A. Baldereschi and N. O. Lipari, Phys. Rev. B **9**, 1525 (1974).
[6] G. L. Bir, E. I. Butikov, and G. E. Pikus, J. Phys. Chem. Solids **24**, 1467 (1963).
[7] K. Suzuki, M. Okazaki, and H. Hasegawa, J. Phys. Soc. Jpn. **19**, 930 (1964).
[8] A. E. Butikov, Fiz. Tverd. Tela (Leningrad) **10**, 3364 (1968) [Sov. Phys. Solid State 10, 2657 (1969)].
[9] P. J. Lin-Chung and R. F. Wallis, J. Phys. Chem. Solids **30**, 1453 (1969).
[10] G. L. Bir and G. E. Pikus, Simmetriya i deformatsionnye effekty v poluprovodnikakh (Symmetry and Deformation Effects in Semiconductors), Nauka, 1972.
[11] B. L. Gel'mont and M. I. D'yakonov, Fiz. Tekh. Poluprovodn. **7**, 2013 (1973) [Sov. Phys. Semicond. **7**, 1345 (1973)].
[12] D. H. Dickey and J. O. Dimmock, J. Phys. Chem. Solids **28**, 529 (1967).
[13] R. A. Faulkner, Phys. Rev. **184**, 713 (1969).
[14] N. Lee, D. M. Larsen, and B. Lax, J. Phys. Chem. Solids **34**, 1817 (1973); **35**, 401 (1974).
[15] N. Lee, D. M. Larsen, and B. Lax, *ibid.*, 1059; P. E. Simmonds, J. M. Chamberlain, R. A. Hoult, R. A. Stradling, and C. C. Bradley, J. Phys. C **7**, 4164 (1974).
[16] A. K. Bhattacharjee and S. Rodriguez, Phys. Rev. B **6**, 3836 (1972).
[17] S. R. Rodriguez, P. Fisher, and F. Barra, Phys. Rev. B **5**, 2219 (1972).
[18] P. Fisher and H. Y. Fan, Phys. Rev. Lett. **2**, 456 (1959).
[19] R. L. Jones and P. Fisher, J. Phys. Chem. Solids **26**, 1125 (1965).
[20] R. L. Jones and P. Fisher, Solid State Commun. **2**, 369 (1964).
[21] R. L. Jones and P. Fisher, Phys. Rev. B **2**, 2016 (1970).

[22]H. P. Soepangkat and P. Fisher, Phys. Rev. B **8**, 870 (1973).
[23]F. I. Sidorov and T. M. Lifshitz, Fiz. Tverd. Tela (Leningrad) **8**, 2498 (1966) [Sov. Phys. Solid State **8**, 3419 (1969)].
[24]T. M. Lifshitz, N. P. Likhtman, and V. I. Sidorov, Pis'ma Zh. Eksp. Teor. Fiz. **7**, 111 (1969) [JETP Lett. **7**, 84, (1969)].
[25]E. E. Haller and W. Hansen, Solid State Commun. **15**, 687 (1974).
[26]M. S. Skolnick, L. Eaves, R. A. Stradling, J. C. Portal, and S. Askenazy, Solid State Commun. **15**, 1403 (1974).
[27]T. M. Lifshitz and F. Ya. Nad', Dokl. Akad. Nauk SSSR **162**, 801 (1965) [Sov. Phys. Dokl. **10**, 532 (1965)].
[28]Sh. M. Kogan and B. I. Sedunov, Fiz. Tverd. Tela (Leningrad) **8**, 2382 (1966) [Sov. Phys. Solid State **8**, 1898 (1967)].
[29]E. M. Gershenzon, L. A. Orlov, and N. G. Ptitsina, Pis'ma Zh. Eksp. Teor. Fiz. **22**, 207 (1975) [JETP Lett. **22**, 95 (1975)].
[30]F. Barra and P. Fisher, Phys. Lett. **27A**, 711 (1968).
[31]H. B. Huntington, Solid State Phys. **7**, Academic Press, New York, 1958, p. 213.

Translated by J. G. Adashko

Distinctive features of order-order type magnetic transitions due to the exchange-striction mechanism

V. I. Val'kov, É. A. Zavadskiĭ, and B. M. Todris

Donets Physico-Technical Institute, Ukrainian Academy of Sciences
(Submitted July 14, 1976)
Zh. Eksp. Teor. Fiz. **72**, 1480–1488 (April 1977)

A technique for computing the P-T phase diagrams of a two-sublattice magnetic substance is developed on the basis of the Bean-Rodbell exchange-striction model. It is shown that, under certain conditions, the Néel temperature T_N can be lower than the temperature at which the energy barrier separating the antiferromagnetic and ferromagnetic phases disappears. In this case the ferromagnetic order should inductively set in near T_N in the sample under investigation. The results of the calculations are confirmed by experiments on the magnetic transitions in manganese arsenide and certain alloys based on this compound. Some new varieties of P-T diagrams of magnetically ordered materials are predicted.

PACS numbers: 75.30.Kz

INTRODUCTION

It has been experimentally established that ferromagnetic ordering in a number of substances is replaced by antiferromagnetic ordering as the temperature is varied.[1–4] Such transitions are usually explained with the aid of Kittel's theoretical model,[5] which is based on the fact that the exchange interaction, linearly varying with the interatomic distance, changes sign at definite, characteristic—for the given substance—dimensions of the crystal lattice. Although Kittel took only one exchange interaction into account in his work, he in fact assumed that there is a second, distance-independent interaction.

Farrel and Meijer[6] took the second coordination sphere directly into account, but considered only the influence of the magnetic field on the equilibrium distances, leaving out of consideration the problems connected with the change of sign of one of the exchange interactions. The calculations in Pal's paper[7] are closest to the real situation, but they were carried out under the assumption that the sublattice magnetization does not change when the ferromagnetic (FM) order is replaced by the antiferromagnetic (AF) order.

As applied to FeRh, which was considered in[7], the above-cited assumption can be considered to be justified. But for a stronger dependence of the exchange interaction on the interatomic distance, the Curie, T_C, or Néel, T_N, temperatures turn out to be different. Then the AF → FM transition temperature can be close to T_N, and the jump occurring in the sublattice magnetization at the time of the transition will be large. This effect has a lesser influence in the inverse FM → AF transition. On the whole then, the $P-T$ phase diagram should change substantially.

In the experimental investigation of the magnetic transitions we encountered in some alloys precisely such a change in the phase diagrams which support the applicability of the above-described approach. Since, in analyzing the results, we found it possible to predict several types of phase diagrams, including FM–AF transitions, it seems to us expedient to generalize the results obtained, which is done in the present paper.

THE THEORETICAL MODEL

The model is based on the assumption that the exchange interaction in both the first, J_1, and second, J_2, coordination spheres depends on the specific volume V. Following Bean and Rodbell's paper,[8] in which an exchange-striction mechanism of phase transitions is developed, we shall assume the dependences $J_1(V)$ and $J_2(V)$ to be linear.

Let the relative disposition of the indicated curves be determined by the parameters indicated in Fig. 1. Let us also introduce the coefficient $n = \partial J_2/\partial V : \partial J_1/\partial V$.

 0038-5646/77/4504-0776$02.40